UCRL-JRNL-201794

Experimental and Theoretical Evaluation of Density Sensitive NVII, ArXIV and Fe XXII Line Ratios

H. Chen, P. Beiersdorfer, L. A. Heeter, D. A Liedahl, K. L. Naranjo-Rivera and E. Trabert M.-F. Gu, J. K. Lepson

January 12, 2004

Submitted to Astrophysical Journal

This work was performed under the auspices of the U.S. Department of Energy by University of California, Lawrence Livermore National Laboratory under Contract W-7405-Eng-48

Experimental and theoretical evaluation of density sensitive N VII Ar XIV and Fe XXII line ratios

H. Chen, P. Beiersdorfer, L. A. Heeter [1], D. A Liedahl,

K. L. Naranjo-Rivera [1] and E. Träbert

High Temperature and Astrophysics Division, Lawrence Livermore National Laboratory, Livermore, CA 94550, U.S.A.

M.-F. Gu

Physics Department, Stanford University, CA 94305, U.S.A.

and

J. K. Lepson

Space Sciences Laboratory, University of California, Berkeley, CA 94720, U.S.A.

ABSTRACT

The line ratios of the 2p-3d transitions in the B-like spectra Ar XIV and Fe XXII have been measured using the electron beam ion traps at Livermore. Radiative-collisional model calculations show these line ratios to be sensitive to the electron density in the ranges $n_e = 10^{10}$ to 10^{12} cm^{-3} and $n_e = 10^{13}$ to 10^{15} cm^{-3}, respectively. In our experiment, the electron beam density of about 10^{11} cm^{-3} was varied by about a factor of 5. Our data show a density effect for the line doublet in Ar XIV, and good agreement with theory is found.

[1]Breck School, Minneapolis, MN 55422, U.S.A.

The relative intensity of the Fe XXII doublet shows good agreement with our predicted low density limit. The N VI K-shell spectrum was used to infer the actual electron density in the overlap region of ion cloud and electron beam, and systematic measurements and calculations of this spectrum are presented as well. The Ar XIV and Fe XXII spectra promise to be reliable density diagnostics for stellar coronae, complementing the K-shell diagnostics of helium-like ions.

Subject headings: :

atomic data - Sun: corona - techniques: spectroscopic

1. Introduction

The evaluation of line intensity ratios as a density and temperature diagnostic is an important topic in plasma physics and astrophysics (Menzel 1969; Kafatos & Lynch 1980; Lynch & Kafatos 1991). The He-like ion forbidden line ($1s2s\ ^3S_1 \rightarrow 1s^2\ ^1S_0$) to intercombination line ($1s2p\ ^3P_1 \rightarrow 1s^2\ ^1S_0$) intensity ratio has long been studied (Gabriel & Jordan 1969; Pradhan 1982) and now is often used as a plasma density diagnostic. In comparison, L-shell ions - which carry rich information on plasma conditions - have been exploited much less because of their more complex atomic structure and more complicated spectral features. For example, studies using iron L-shell lines in the EUV (at wavelengths of about 100 Å) for density determinations of the coronae of a stellar binary (Brickhouse & Dupree 1998) have produced densities estimate with an uncertainty of two orders of magnitude.

In order to extract plasma information more precisely from L-shell spectral data, it is very desirable to utilize data from a variety of atomic systems and elements, and in several wavelength ranges. Among the simplest systems with density sensitive L-shell lines are B-like ions. Because high resolution spectral data was available only for the Sun, this ionic system has been studied mostly for solar data until recently. For example, calculations for the density sensitive iron L-shell $3 \rightarrow 2$ lines were made (Doschek et al. 1973) to determine the plasma density from high-resolution solar flare observations and controlled fusion plasmas. These were followed by more detailed calculations (Mason & Storey 1980). Observations of the Fe XXII lines from solar flares have also been presented (Phillips et al. 1982, 1996; Fawcett et al. 1987). A comparison of these observations to theoretical calculations indicated the need for a revision of the latter. In addition, the 2p-4d lines in Fe XXII were discussed (Wargelin et al. 1998) in the analysis of tokamak data. Now that high-resolution data are being obtained by current space X-ray observatories, interest is renewed for using L-shell ions as plasma diagnostics. For example, using *Chandra* High-Energy Transmission Grating

data, Mauche, Liedahl and Fournier have applied $3 \rightarrow 2$ line ratios of Fe XVII (Mauche et al. 2001) and Fe XXII (Mauche et al. 2003) to constrain and derive the density of the magnetic cataclysmic variable EX Hydrae.

In this paper, we present detailed studies on the density dependent boron-like argon and iron, as well as helium-like nitrogen systems. These ion species are suitable probes for the density range of astrophysical interest ($n_e = 10^{10}$ to 10^{15} cm^{-3}). We have performed model calculations of the line ratios as a function of density using the Flexible Atomic Code (FAC) (Gu 2003) as well as using the Hebrew University Lawrence Livermore Atomic Code (HULLAC) (Bar-Shalom et al. 2001). We experimentally tested the code predictions using the university of California Lawrence Livermore National Laboratory (LLNL) electron beam ion traps.

2. Boron-like ion density diagnostic model

The density sensitive lines of primary interest in boron-like ions are those of the 2p-3d transition multiplet. Their intensity ratio depends on the 2p ground state level populations from which collisional excitation takes place. At low densities, the true ground level $1s^2 2s^2 2p_{1/2}\ ^2P_{1/2}$ is almost exclusively populated, whereas the population of the upper (metastable) level of the ground term, $1s^2 2s^2 2p_{3/2}\ ^2P_{3/2}$, is insignificant. All ions in the upper level have time enough between collisions to decay towards the true ground level. The 3d levels are even shorter-lived by many orders of magnitude. At the high density limit, the population ratio of the $2p_{1/2}$ and $2p_{3/2}$ levels reflects the local thermal equilibrium and thus approaches the statistical ratio 1:2. In between these limits, the population ratio reflects the density of the plasma. The decisive parameter for this process is the radiative lifetime in comparison to the typical time between collisions (Menzel 1969). For Ar XIV, the lifetime of the metastable level has been measured as 9.70 ms (Träbert et al. 2000). For Fe, we have

calculated a metastable level lifetime of 0.068 ms. By measuring the ratio of the 2p-3d lines, which are mostly excited from the two fine structure levels of the ground term (Fig. 1), we can obtain density information on the plasma.

For Ar XIV, the 2p-3d lines lie in the soft-x-ray spectrum, at wavelengths of 27.469 Å and 27.631 Å, respectively (Lepson et al. 2003), while for Fe XXII, the lines are at wavelengths more than a factor of two shorter at 11.770 Å and 11.946 Å(Brown et al. 2002).

An evaluation of the line ratios in terms of plasma density, however, requires much more information than the line wavelengths (for identification) and the metastable level lifetime (for a crude estimate of the range of applicability). In fact, many levels can be collisionally excited and deexcitated by various channels and these processes can repopulate the 3d levels of interest here. Most of these transitions are outside our spectral detection range, and thus theory is needed to model the system. In the calculations with FAC, B-like Ar and Fe models contain all energy levels accessible with one-electron excitation from n=2 orbital to n'$\leq$ 10 orbital. Electron collisional excitation from the n=2 configurations are calculated with the relativistic distorted-wave approximation implemented in FAC. All E1 radiative transitions between n' $\rightarrow$ n are included for all possible n' and n. For n' $\rightarrow$ n with n' $\leq$ 3, E1, M1, E2, and M2 transitions are included. Level populations are obtained in the steady state condition for different electron densities, which are then used to compute line emissivities. In these models, only direct excitation is accounted for, and resonant excitation effects are not included. However, at the electron beam energies used in our measurements, such resonance contributions are expected to be negligible.

Figure 1 indicates the FAC results for the branching fractions for excitation and de-excitation within the 2p-3d multiplet of Ar XIV. The basic atomic structure information is then used in the collisional-radiative modeling process. The model indicates a low density limit for Ar at $n_e < 2 \times 10^{10}$ cm^{-3} and a high density limit at $n_e > 10^{13}$ cm^{-3}. In the

case of B-like Fe, the low density limit is at $n_e < 2 \times 10^{12}$ cm^{-3}, while the high density limit is at $n_e > 5 \times 10^{15}$ cm^{-3}. As is expected from the metastable level lifetime, higher-Z ions are suitable as density diagnostics at higher densities. Both of the above ranges match conditions that are known to appear in various stellar objects.

3. Laboratory measurements

To evaluate our predictions, we made measurements at the LLNL electron beam ion traps. For part of the work, the SuperEBIT device was reconfigured to permit high electron beam currents at the rather low electron beam energies needed here, and for the other part, the EBIT-I (low-energy) electron beam ion trap was used (Levine et al. 1988). The magnetic field strength of the super conducting magnets of the electron beam ion trap was 3 T; this field was needed to squeeze the diameter of an electron beam to about 60 μm in order to reach a high current density, and to guide the beam through a set of drift tubes that act as a Penning ion trap. Soft X-ray photons of interest were dispersed and observed by using two flat-field grating spectrometers equipped with a 2400 ℓ/mm variable line spaced concave grating (Harada & Kita 1980) and a cryogenically cooled back-thinned CCD detector. One CCD camera had a detector chip with 1024×1024 pixels on a square area of 25 mm edge length, the other camera chip had 1300×1340 pixels on a similar area.

Argon spectra were recorded at electron beam energies from 1 keV to 3.2 keV, and at electron beam currents in the range from 0.3 mA up to 135 mA. For the measurements of iron, the electron beam energy range was 1.7 keV – 4.5 keV, with electron beam currents ranging from 10 to 90 mA. Measurements of the K-shell emission of nitrogen were made to calibrate the electron density, as described in the next section.

Well over 100 CCD spectral images were taken, requiring 20 to 60 minutes of exposure

time each. Spectra recorded under similar experimental conditions were summed to improve the counting statistics and the signal-to-noise ratio. Spectra obtained with an 'inverted trap' (Utter et al. 2000) helped to determine the background shape of the CCD spectra which is needed for a proper determination of the intensities of the spectral lines. An example of an Ar spectrum together with a nitrogen calibration spectrum is shown in Fig. 2.

3.1. Electron density determination

By varying the electron beam current we varied the electron density in the trap. Figure 3 shows the density sensitive B-like Ar lines observed at different beam currents. It is easily seen that the line intensity ratio R, defined as

$R = (I_{(3d_{5/2} \rightarrow 2p_{3/2})} + I_{(3d_{3/2} \rightarrow 2p_{3/2})})/I_{(3d_{3/2} \rightarrow (2p_{1/2})}$,

varies as a function of the electron beam current. However, the relation between electron beam current and density is not easily determined and need not be linear. In all of our spectra, line $3d_{3/2} \rightarrow 2p_{1/2}$ is well resolved, while the two lines $3d_{5/2} \rightarrow 2p_{3/2}$ and $3d_{3/2} \rightarrow 2p_{3/2}$ are not resolved from each other. This, however, does not affect our results, because the line ratio R defined above involves the sum of the intensities of these two lines.

The upper limit of the electron density in the trap can be estimated by assuming that the electron beam from the electron gun upon entering the high B-field region is squeezed to a diameter of about 50 μm (Levine et al. 1988). In such a scenario, the electron beam current would be directly proportional to the electron density. From this simple geometric argument, an electron density of about 3×10^{10} cm^{-3} to 3×10^{13} cm^{-3} is expected for electron beam currents ranging from 0.3 to 130 mA. In reality, the effective electron density will be smaller than this estimate, because the ions gyrate and oscillate in the electromagnetic field and thus move in and out of the electron beam.

We can crudely estimate the lower limit of the electron density in the trap using a simple model that neglects the attraction by the electric field of the beam electrons. Assume each ion passes the electron beam once. The fraction of electron density f seen by the ions can be estimated as the ratio of the beam diameter d_{beam} and the circumference of the ion gyromotion: $f = d_{beam}/(2\pi(2m_iT_i)^{1/2}/(eB))$. Given d_{beam} is about 50 μm, the ion temperature T_i is about 100 eV and the magnetic field strength B is 3 Tesla, we estimated an overlap of 0.5% between the electron beam and the trapped ion cloud. That result in an effective electron density of 0.5% of the aforementioned maximum. The complexity of the ion electron interaction processes makes it difficult to know accurately the level of overlap, which varies as a function of many parameters such as ion charge, the ion temperature, and the electron space charge. For example, DeWitt et al. estimated the overlap to be about 15% level (Dewitt et al. 1991) in a previous measurement on the Livermore EBIT-II electron beam ion trap.

In order to determine the electron density more precisely, we performed measurements of the intensity ratio of the He-like nitrogen (N VI) "y" and "z" lines ($1s^2\ ^1S_0$ - $1s2p\ ^3P_1$ and $1s^2\ ^1S_0$ - $1s2s\ ^3S_1$, respectively). A discussion of the identity of the line z, which generally is weak at typical electron beam ion trap densities was given earlier by Beiersdorfer et al. (1999) The density effect on the "y" and "z" lines is evident in our data (Fig. 4).

The use of the z/y line ratio as a density diagnostic has been investigated by Gabriel & Jordan (1969); Pradhan & Shull (1981); Pradhan (1982). In the present study, we calculated the nitrogen electron excitation and radiative decay rate coefficients, and computed the N VI line intensities as a function of electron density using the collisional radiative model included in the FAC code. We did this for each electron beam energy for which we had experimental data. The cascade contributions to the excitation rates were included. The results are plotted in Fig. 5. Here we plotted the electron density as a function of the line ratio, as

we use the results to infer the electron density from the measured line ratios. The figure also shows the experimental line ratios from nitrogen. Those values were corrected for the polarization (Beiersdorfer et al. 1996) that is caused by the mono-directional electron beam. From the line ratios (x axis), we can determine the electron density (y-axis) in the electron beam ion trap with reference to the theoretical expectations. The error bars refer to the uncertainties in the measurements.

Furthermore, using the nitrogen line ratio data, we can infer the relation between the electron beam current and the electron density. In theory, $I_{beam} = e \times n_e \times A \times v_e$, where A is the cross section of the beam, and v_e is the velocity of the electrons at energy E. Therefore $I_{beam}/(e \times E^{1/2}) = n_e \times C$, where C is some constant depending on the beam radius. Assuming that the beam radius is constant during the experiment, we can expect a linear dependence of n_e over $I_{beam}/E^{1/2}$. This dependence is indeed seen (Fig. 6). However there is quite some scatter. Scatter might result from variations of the electron density across the beam profile, or from variations in beam radius during the experiment. But these effects are likely to be minor (Savin et al. 2000). The most likely reason for the scatter is the variation in the beam-ion overlap caused by varying amounts of space charge neutralization that changes the effective electron density seen by the ions.

The electron density derived from the measurements with nitrogen is in the range between the maximum and minimum estimates from our crude estimates, and the measured density variation is much smaller (by a factor of 5 - 10, depending on the beam current value) than might be expected from the variation of the electron beam current alone. From these experiments, it is clear that an experimental calibration of the density in the electron beam ion trap is needed before the density dependence of the Ar XIV and Fe XXII line ratios can be verified. Using the experimentally established relation of n_e vs $I_{beam}/E^{1/2}$, we can derive the electron density for every B-like line ratio measurement at its beam current and density.

This approach assumes that the beam-ion overlap for Ar XIV and Fe XXII follows similar variations as that for N VI. While this may not be true in all case, it so far provides us with the best estimate of the electron density for our line ratio measurements.

4. Line ratio results

The results of the B-like Ar XIV line ratio measurements are compared to the predictions from the FAC calculations in Fig. 7. At an electron energy of 1 keV, the agreement between experimental data and prediction is good. A slight disagreement between prediction and experiments appears in the data recorded at higher density ($n_e > 2 \times 10^{11}\mathrm{cm}^{-3}$), where the experimental data indicate a $20\% - 30\%$ higher density, or a $10\% - 20\%$ lower line ratio, than the prediction does. We note that similar to the FAC results for N VI, there is very little difference in the curves calculated for a monoenergetic beam and for a thermal plasma. This indicates that our results obtained with a largely monoenergetic electron beam are applicable to thermal plasmas.

A typical Fe spectrum with the Fe XXII lines of present interest is shown in Fig. 8. The Fe predictions obtained by using the FAC and HULLAC codes, respectively, agree very well, as is seen in Fig. 9. Both calculations agree in showing a low density limit of less then 5×10^{12} cm^{-3}. All our electron beam currents correspond to an electron density of $< 2 \times 10^{12}$ cm^{-3} (see Fig. 6), which is at the low density limit of this curve. Measured data and predictions are in excellent agreement, as shown in (Fig. 9). In fact, both HULLAC and FAC predict 0.33 as the low density ratio. This compares well to the value of 0.32 ± 0.01 which results from the weighted average of all of our experimental data from EBIT-I.

In summary, B-like ion line ratios for Ar and Fe have been studied as a function of electron density both theoretically and experimentally. Within the electron density range

obtained in our electron beam ion trap, prediction and measurement are in good overall agreement. Our modelling effort and experimental validation of the B-like Ar and Fe ionic systems provide a valuable diagnostic tool to laboratory plasma physics and astrophysics.

5. Acknowledgments

The work at the University of California Lawrence Livermore National Laboratory was performed under the auspices of the Department of Energy under Contract No. W-7405-Eng-48 and supported by NASA Space Astrophysics Research and Analysis work order W19, 878. E.T. acknowledges travel support by the German Research Association DFG.

REFERENCES

Bar-Shalom, A., Klapisch, M., & Oreg, J. 2001, J. Quant. Spec. Radiat. Transf., 71, 169

Beiersdorfer, P., Vogel, D. A., Reed, K. J., Decaux, V., Scofield, J., Widmann, K., Hlzer, G., Frster, E., Wehrhan, O., Savin, D. W., & Schweikhard, L., 1996 Phys. Rev. A 53 3974-3981

Beiersdorfer, P., Crespo Lpez-Urrutia, J. R., Springer, P., Utter, S. B., & Wong, K. L., 1999, Rev. Sci. Instruments 70, 276-279

Brickhouse, N. S. & Dupree, A. K., 1998, ApJ, 502, 918

Brown, G. V., Beiersdorfer, P., Liedahl, D. A., Widmann, K., Kahn, S. M. & Clothiaux, E. J., 2002, ApJS, 140, 589 (Note: in Table 7 of this paper, the identification of B9 line should be C13 (11.977 Å), and B9 transition is blended into B10 - Private communication with G. V. Brown, 2003.)

DeWitt, D. R., Schneider, D., Clark, M. W., & Chen, M. H., 1991, Phy. Rev. A, 44, 7185

Doschek, G. A., Meekings, J. F., & Cowan, R. D., 1973, Sol. Phys., 29, 125

Drake, G. W. F. 1988, Can. J. Phys., 66, 586

Fawcett, B. C., Jordan, C., Lemen, J. R., & Phillips, K. J. H. 1987, Mon. Not. R. astr. Soc., 225, 1013

Gabriel, A. H. & Jordan, C. 1969, MNRAS, 145, 241

Garcia, J. D. & Mack, J. E. 1965, J. Opt. Soc. Am., 55, 654

Gu, M. F. 2003, ApJ, 582, 1241

Harada, T. & Kita, T. 1980, Appl. Opt., 19, 3987

Kafatos, M. & Lynch, J. P. 1980, ApJS, 42, 611

Lepson, J. K., Beiersdorfer, P., Behar, E., & Kahn, S. M. 2003, ApJ, 590, 604

Levine, M. A., Marrs, R. E., Henderson, J. R., Knapp, D. A., & Schneider, M. B. 1988, Phys. Scr., T, 22, 157

Lynch, J. P. & Kafatos, M. 1991, ApJS, 76, 1169

Mason, H. E. & Storey, P. J., 1980, MNRAS, 191, 631

Mauche, C. W., Liedahl, D. A., & Fournier, K. B. 2001, ApJ, 560, 992

Mauche, C. W., Liedahl, D. A., & Fournier, K. B. 2003, ApJ, 588, L101

Menzel, D. H. 1969, Mem. Soc. R. Sci. Liège, 17, 113

Phillips, K. J. H., Leibacher, J. W., Wolfson, C. J., Parkinson, J. H., Fawcett, B. C., Kent, B. J., Mason, H. E., Acton, L. W., Culhane, J. L., & Gabriel, A. H., 1982, ApJ, 256, 774

Phillips, K. J. H., Bhatia, A. K., Mason, H. E., & Zarro, D. M., 1996, ApJ, 466, 549

Pradhan, A. K. 1982 ApJ, 263, 477

Pradhan, A. K. & Shull, J. M. 1981, ApJ, 249, 821

Savin, D. W., Beiersdorfer, P., Kahn,S. M., Beck, B. R., Brown, G. V., Gu, M. F., Liedahl, D. A., & Scofield, J. H., 2000, Rev. Sci. Instrum., 71, 3362

Träbert, E., Beiersdorfer, P., Utter, S. B., Brown, G. V., Chen, H., Harris, C. L., Neill, P. A., Savin, D. W., & Smith, A. J. 2000, ApJ, 541, 506

Utter, S. B., Beiersdorfer, P., & Brown, G. V. 2000, Phys. Rev. A, 61, 030503

Wargelin, B. J., Beiersdorfer, P., Liedahl, D. A., KAHN, S. M., & Von Goeler, S. 1998, APJ, 496, 1031

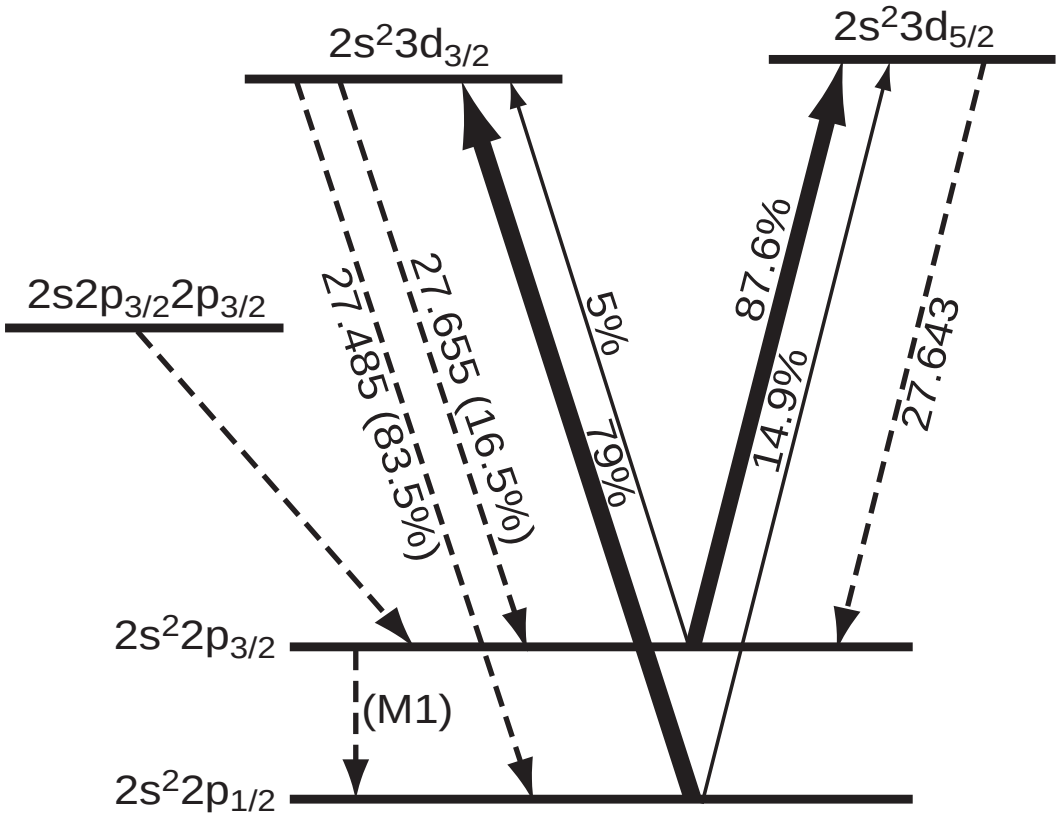

Fig. 1.— Schematic diagram of atomic processes responsible for the density sensitive Boron-like 3 → 2 transitions in Ar XIV. Wavelengths (in Å) and radiative branching fractions (percentages in parentheses, if less than 100%) are given for the radiative transitions (dotted lines). Relative magnitudes of collisional excitation rate coefficients are given in percent as well as represented by the thickness of the solid lines. The numbers given in the figure are for $n_e = 5 \times 10^{11}$ cm^{-3}.

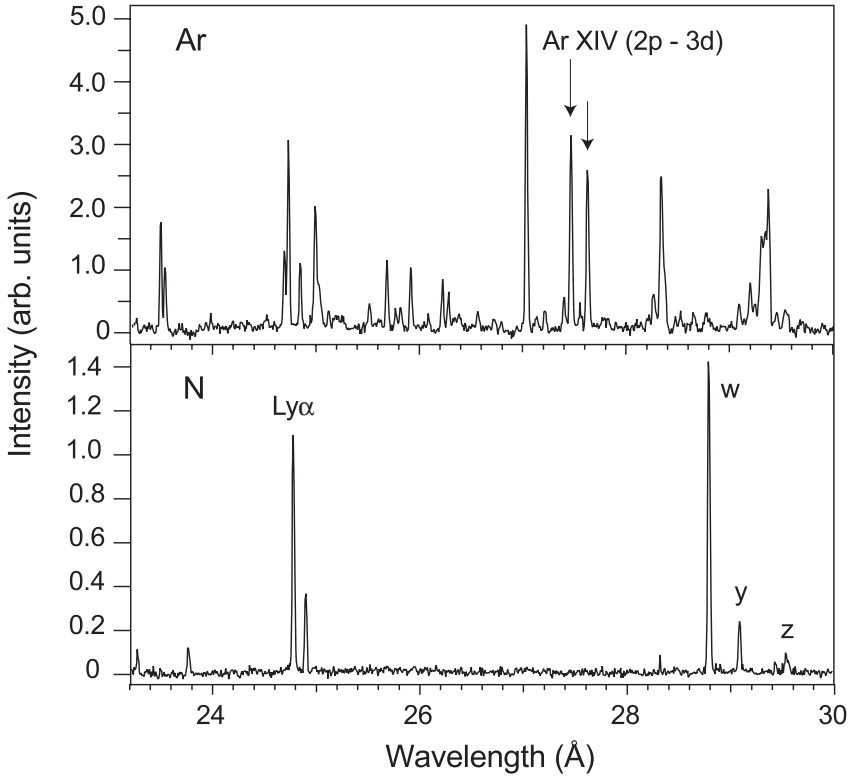

Fig. 2.— EUV spectra of Ar and N recorded with a flat-field grating spectrometer. Both spectra shown were produced at 1 keV electron beam energy. The Ar XIV lines of present interest are marked.

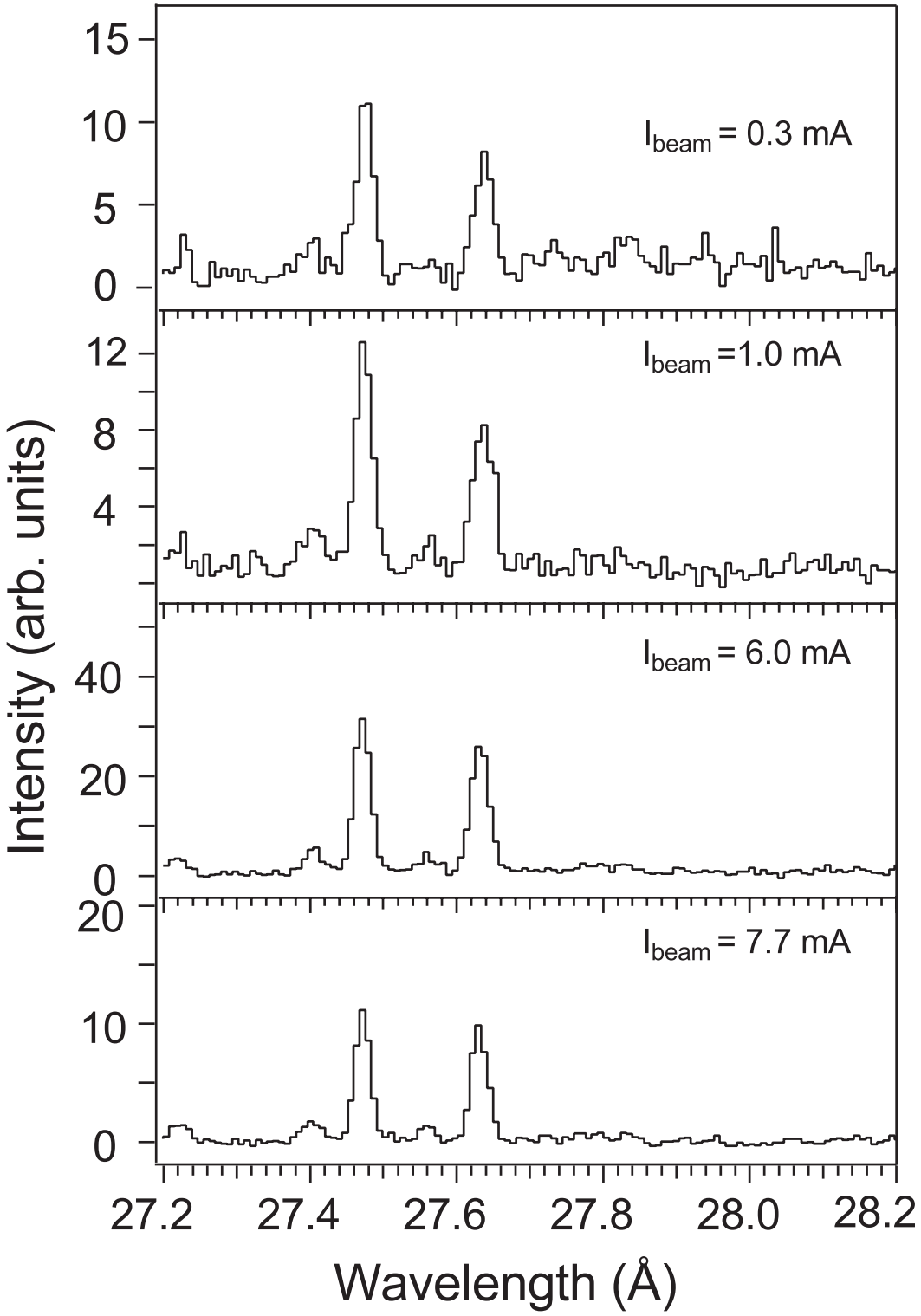

Fig. 3.— Ar spectra at four electron beam currents, showing the Ar XIV $(3d_{3/2} \rightarrow (2p_{1/2})$ transition at 27.47 Å and the Ar XIV $(3d_{5/2} \rightarrow 2p_{3/2})$ and $(3d_{3/2} \rightarrow 2p_{3/2})$ transitions at 27.63 Å.

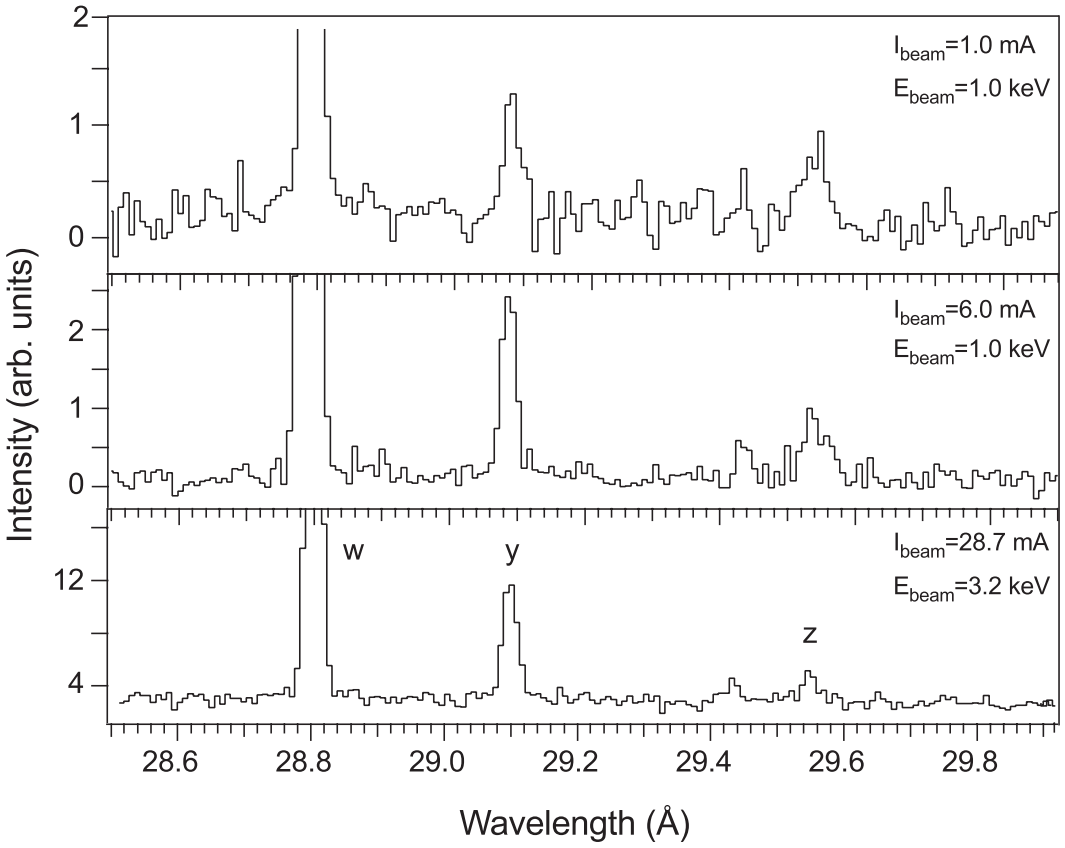

Fig. 4.— N spectra at three electron beam currents, showing the three 1 - 2 transitions "w", "y", and "z" of N V. The "y" vs. "z" line ratio is used as an electron density diagnostic for the electron beam ion trap.

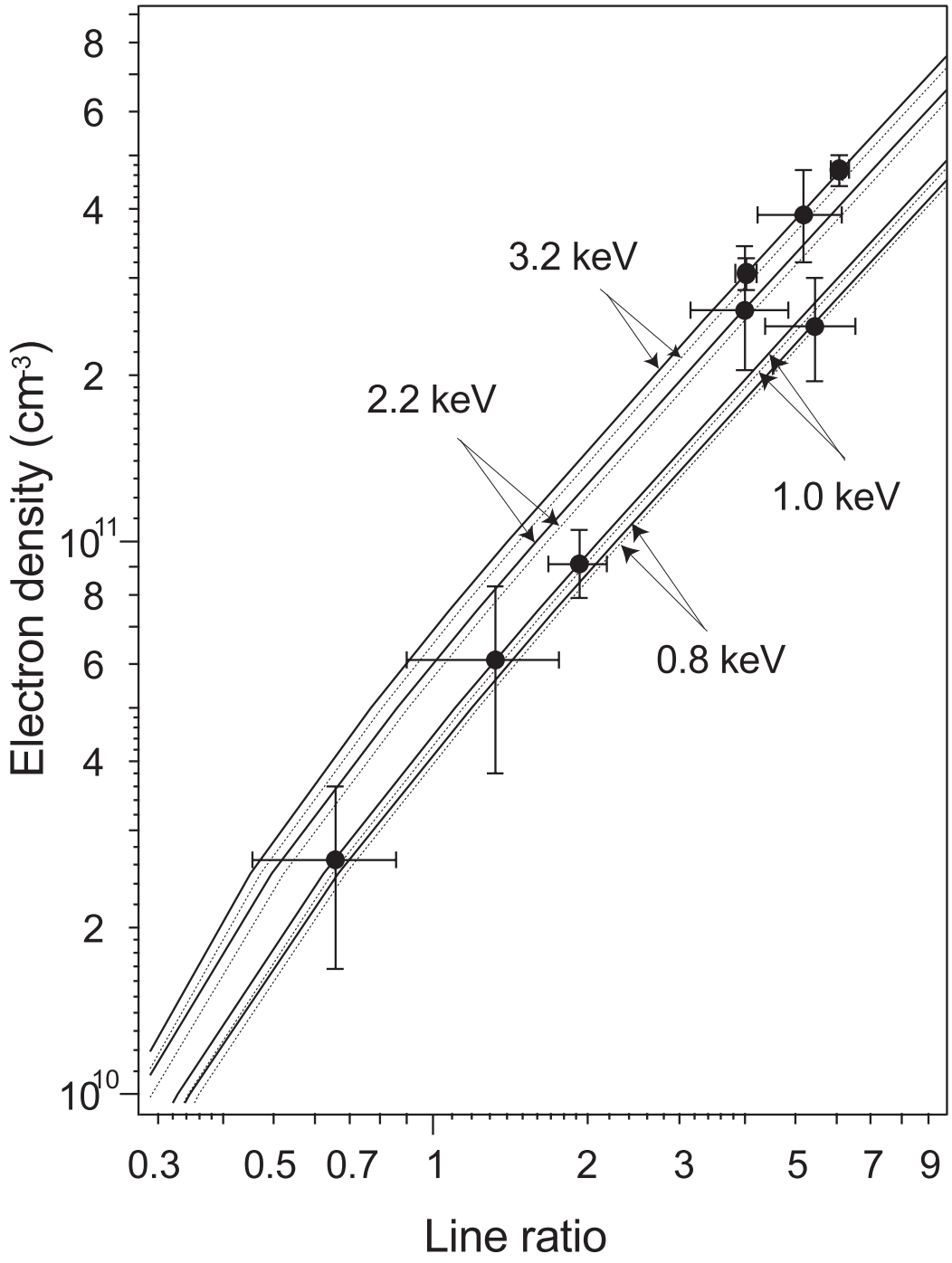

Fig. 5.— Nitrogen line ratios as a function of electron density from FAC code calculations for different electron beam energies and electron temperatures. The solid lines are FAC calculations for the monoenergetic electron beam and the dotted lines for the Maxwellian electron distributions.

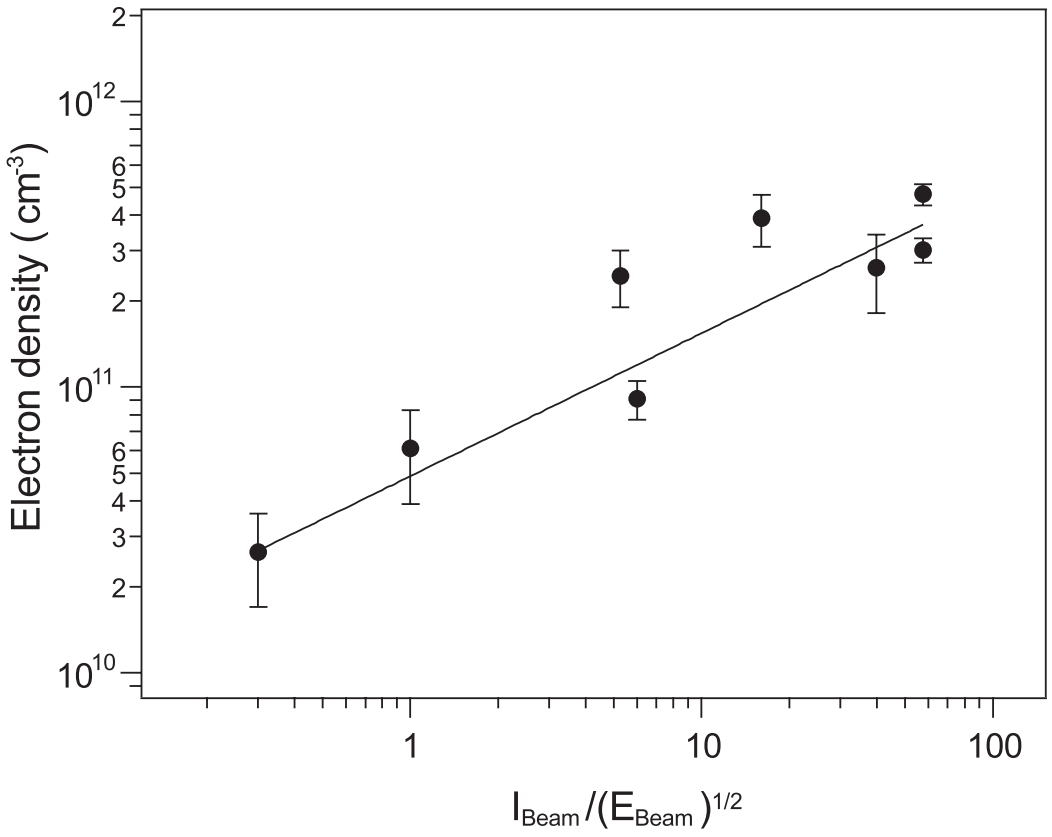

Fig. 6.— Electron density in the electron beam ion trap as a function of electron beam current corrected for electron energy effect from N measurements. The dots indicate electron density values inferred from nitrogen line ratio measurements. The line is the fit (powerlaw) to the data.

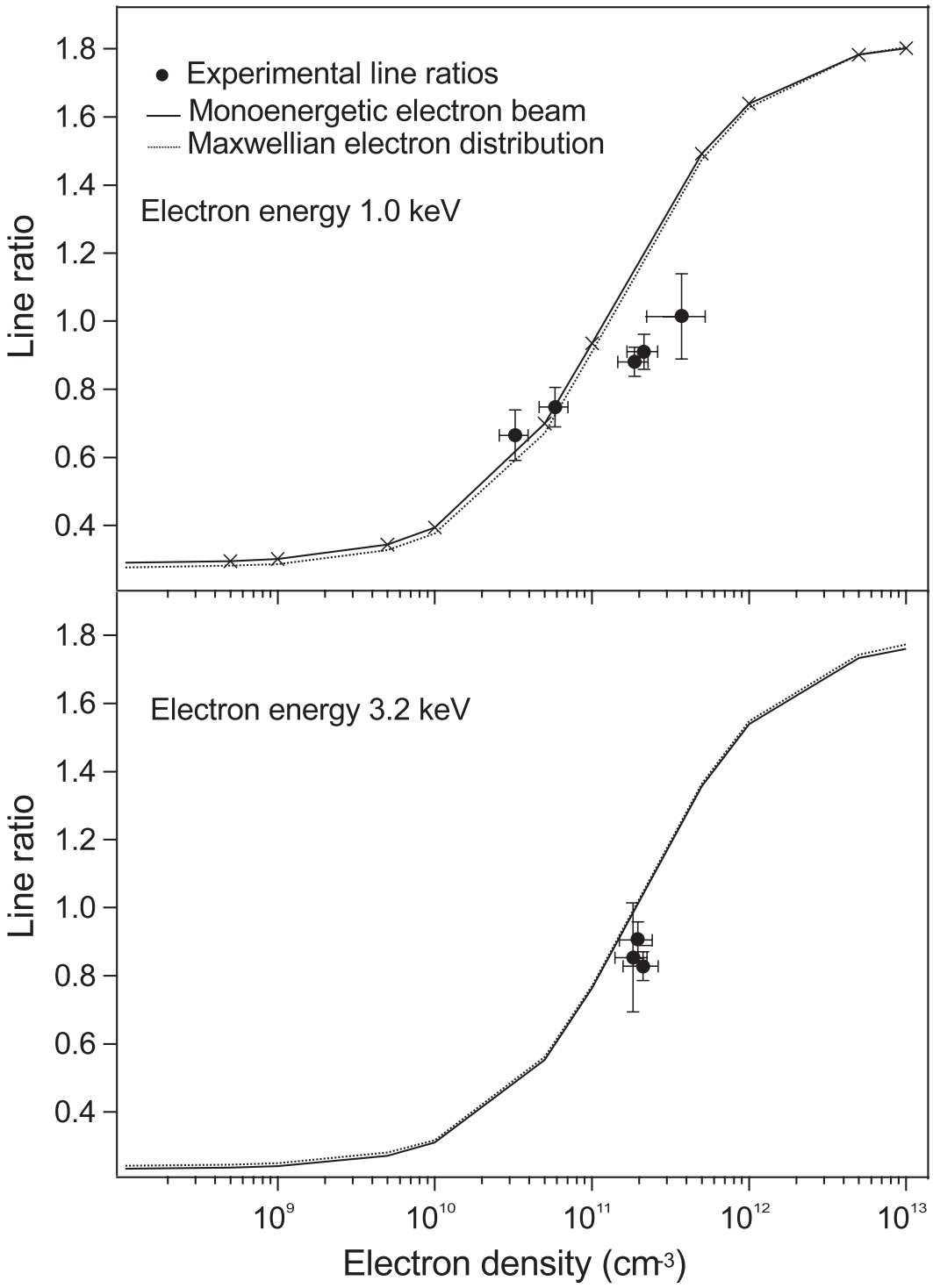

Fig. 7.— Comparison of measured and calculated Ar XIV 3d →2p line ratios as a function of electron density. The upper figure is for an electron beam energy of 1.0 keV, and the lower figure for an electron beam energy of 3.2 keV. Calculations are for both a monoenergetic beam (solid line) and a thermal Maxwellian plasma (dotted line).

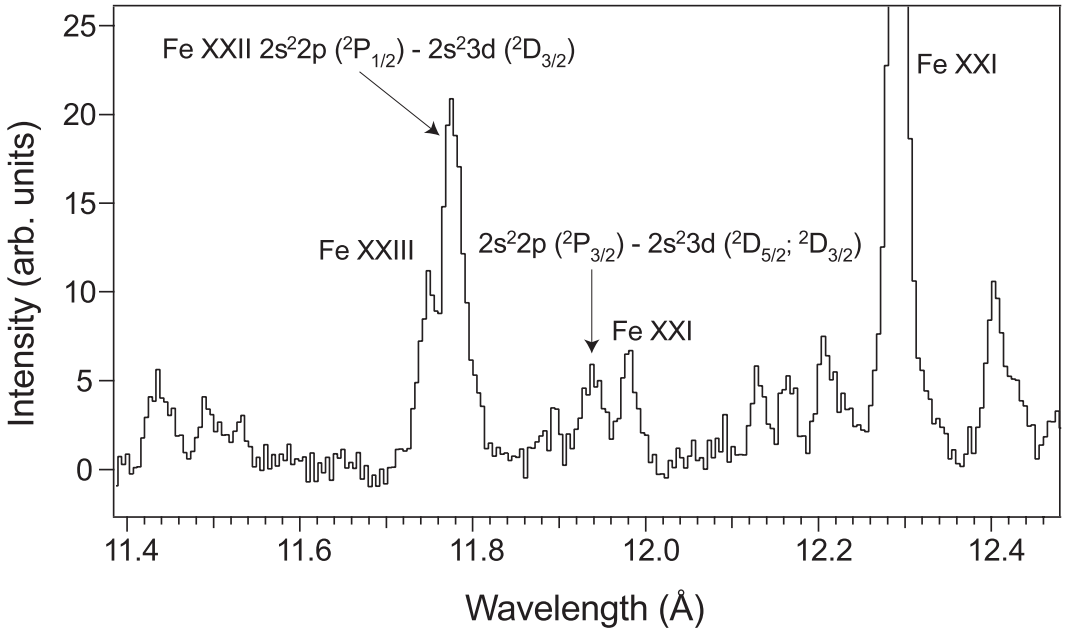

Fig. 8.— Fe spectrum obtained with the grating spectrometer at an electron beam energy of 2.1 keV. The density-sensitive Fe XXII 3d → 2p lines are marked.

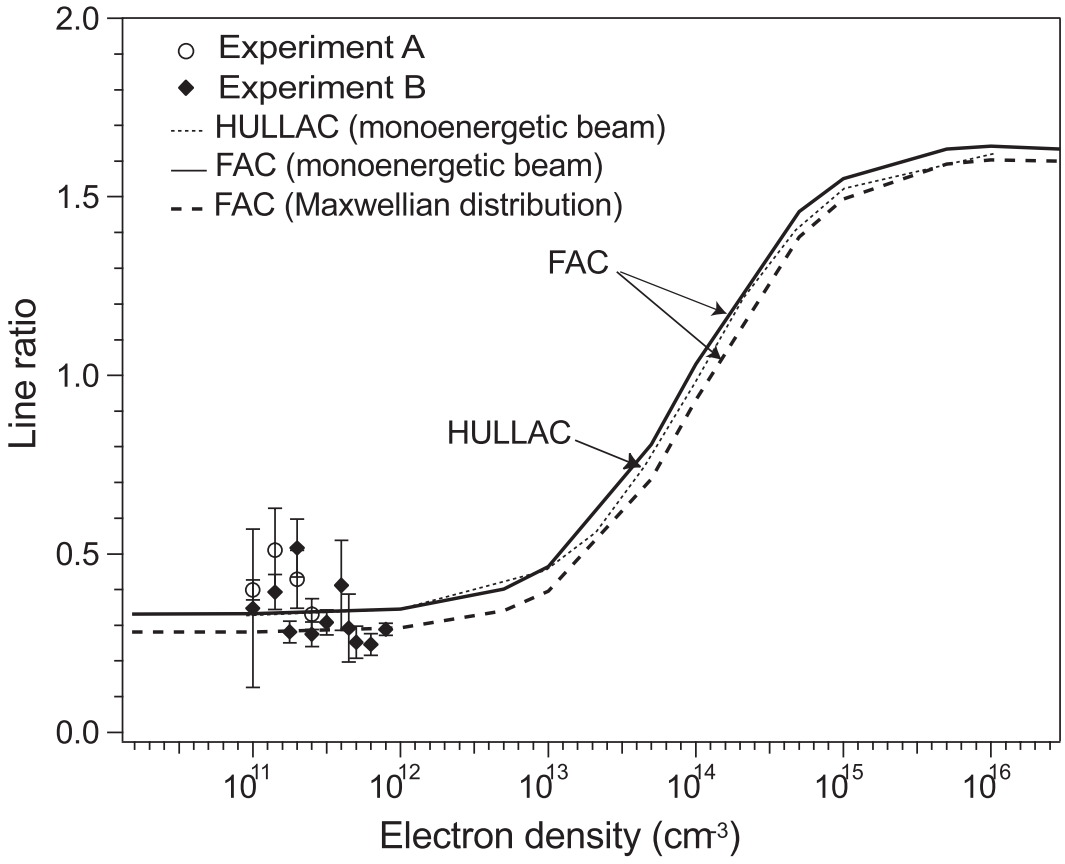

Fig. 9.— Comparison between measured and calculated Fe XXII 3d →2p line ratio values as a function of electron density at an electron beam energy of 2.1 keV. The data shown are from two sets of separate measurements. For better readability, these data are displayed over a wider range of low densities than achieved in the experiment; this seems justified since theory shows no variation in this range.

University of California
Lawrence Livermore National Laboratory
Technical Information Department
Livermore, CA 94551